Plasmonic Halos – Optical Surface Plasmon Drumhead Modes

(Supplemental Information)

Fan Ye, Michael J. Burns, and Michael J. Naughton

Department of Physics, Boston College, 140 Commonwealth Avenue, Chestnut Hill, MA 02467

Additional details of transmission spectra contour map

The relationships between the free-space electromagnetic wavelength λ_0 and the SPP wavelengths λ_{SPP} along the Ag/air and Ag/PMMA interfaces are obtained via the formula $\lambda_{SPP} = \lambda_0 \sqrt{(\varepsilon_0 + \varepsilon_{Ag})/\varepsilon_0 \varepsilon_{Ag}}$, where the ε's are the frequency-dependent complex relative dielectric functions for the respective materials. Plotted in Figure S1, these results are used below when interpreting the dependence of transmission on cavity side wall height.

With this, we can now plot the measured transmission spectrum *vs.* SPP wavelength at the Ag/air interface, for various cavity radii. Figure S2 shows some examples of the normalized transmission spectrum at selected radii, corresponding to a straight dashed line in the contour map. The normalization is obtained by first dividing the transmission spectrum data measured on the completed samples by that through a blank ITO-glass substrate, and then dividing this ratio by a fill factor for each sample. The fill factor is calculated as $F = \pi d(2R_o+d)/a^2$, where a = 10 μm is the distance between neighboring circular holes, R_o the radius of the hole, and d = 300 nm is the width of the taper at the perimeter of the Ag disks. Thus, F represents the fill factor of a unit cell of size a^2 containing a circular annulus of inner radius R_o and width d.

Origin of bands of suppressed vertical transmission

Using the above information, we plot in Figure S3a the measured transmission spectrum *vs.* SPP wavelength at the Ag/PMMA interface (as opposed to the Ag/air interface plot in Figure 2b), for various cavity radii. As indicated in the figure, regions or bands of suppressed transmission appear near SPP wavelengths of 200 nm, 270 to 300 nm and above about 400 nm. After using focused ion beam milling to expose the cavity edge and allow a measurement of the cavity's Ag sidewall height, obtaining h = (400 ± 9) nm, we noted an empirical relationship between this height and the above wavelengths: $h \sim \ell\, \lambda_\ell/2$. That is, it appears that far field scattering at the perimeter of the cavity (the halos) is suppressed for SPP wavelengths $\lambda_\ell = 2h/\ell$ = 400, 267 and 200 nm, for ℓ = 2, 3 and 4, respectively, or whenever the side wall height is integer times half the SPP wavelength along the Ag/PMMA interface.

To confirm this origin of suppressed transmission bands, finite element electromagnetic simulations were carried out for a manageable facsimile of the experimental circular cavity/trench: an infinitely long trench with the same cross-section as the circular plasmonic cavity. That is, choosing a linear trench structure greatly reduces computation time, while still capturing the essential physics. Results are shown in Figure S3b. The height of the PMMA layer is set at 400 nm in the simulation. Trench widths are tuned from 2 to 4 μm, in 50 nm increments, mimicking the range of experimental circular cavity diameters. Optical throughput intensity is obtained by integrating the time-averaged energy density in perfectly matched layers in the far field. Three bands of suppressed transmission appear in the simulated transmission spectra, centered at 200 nm, 267 nm, and 400 nm, close to the experimentally-observed ℓ = 4, 3 and 2 bands above.

In careful examination of the simulated electric field profiles as shown in Figure S4, one can see the origin of this suppression: standing SPP waves develop along the Ag/PMMA interface at these resonant conditions. For example, in the 400 and 267 nm simulations, E_x is seen to possess ℓ=2 and ℓ=3 antinodes, respectively. As E_x corresponds to a wavevector k_z (upwards in the figure), these resonances represent conditions where incident optical energy is converted to plasmonic energy in the trench sidewall, and thus not transformed/scattered back into optical energy that can propagate into the far field along z (*i.e.* as the halo effect). Note that due to the verticality of the side wall, E_x, rather than E_z, represents the TM component to the field here. An off-resonance example, λ_{SPP}=320 nm, is also shown in Figure S4, highlighted by the red box. Here, transmission through the side wall is high, relative to the resonant conditions.

To confirm the ability of the PMMA thickness and thus sidewall height h to tune far field transmission, arrays of plasmonic cavities with radii between 2 and 3 μm were fabricated on a PMMA layer with linearly varying height t_P, as described in detail in Figure 4 in the main text (shown again here as Figure 5Sa). FEM simulation results on the trench facsimile, with tuning geometry to mimic the fabricated circular SPP cavities, are shown in Figure S5b. The simulations are done for trench widths from 2.0 to 3.0 μm, and t_P periodically oscillating (as in Figure 4a) between 508 and 550 nm. We ascribe the fact that the tilting bands on the right side of the figure are larger than in the measured case to the geometry difference between a 1D trench and a 2D circle. A clear zig-zag shape can be seen from the vertical bands of the simulated spectrum map, mimicking the behavior of the vertical band from the measured spectrum map. This confirms the role of side wall height in the modulation of transmission.

Fabrication details for Figure 1c

Fabrication details for Figure 1c are as follows. Starting from the red ring on the left to right, the radii R_o (μm) and electron-beam writing dosages D (μC/cm^2) for the composite circular cavities are: (R_o, D) = (3.5, 375), (3.0, 525), (2.8, 325), (2.2, 525), and (1.8, 375), respectively. The silver sputtering deposition time is 9 min for the second and fourth rings, and 8 min for the others.

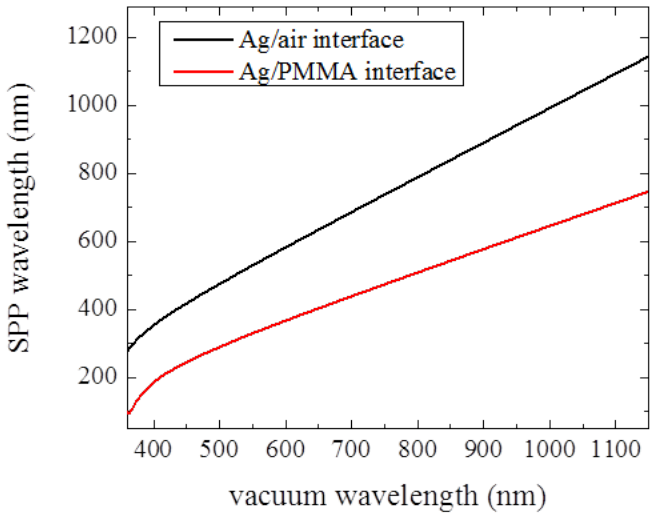

Figure S1. Calculated SPP wavelength along Ag/air and Ag/PMMA495 interfaces *vs.* vacuum (free space) wavelength.

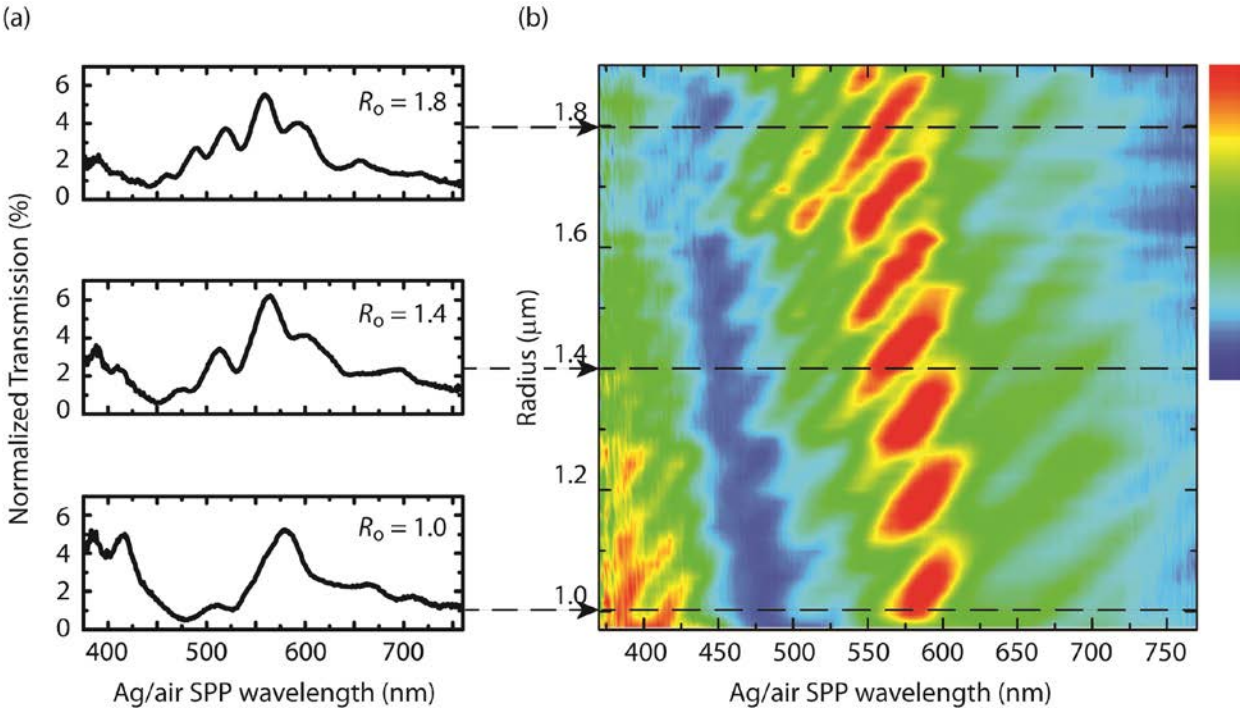

Figure S2. (a) Normalized transmission *vs*. SPP wavelength along Ag/air interface for drumhead cavities with selected radii. (b) Normalized transmission spectrum contour map as shown in Figure 2b, with a linear color bar ranges from 0 to 6%. Note that to emphasize the drumhead mode branches, all transmission larger than 6% is cut off and represented by red color.

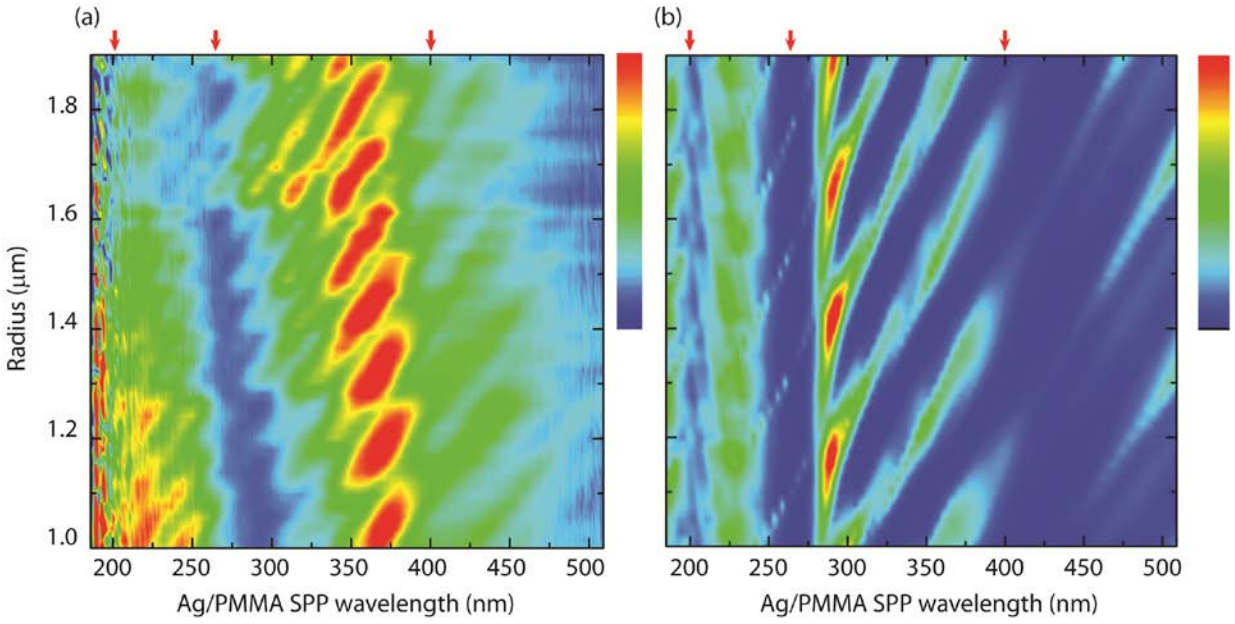

Figure S3. (a) Measured transmission spectra of circular plasmonic cavity arrays *vs.* SPP wavelength at the Ag/PMMA interface when tuning cavity radius from 1.0 to 1.9 μm, in 20 nm increments. (b) Simulated transmission energy through a closely-related linear trench structure *vs.* SPP wavelength at a Ag/PMMA interface. Trench widths are tuned to resemble circular cavity radii from 1.0 to 1.9 μm. Red arrows indicate positions of transmission suppression.

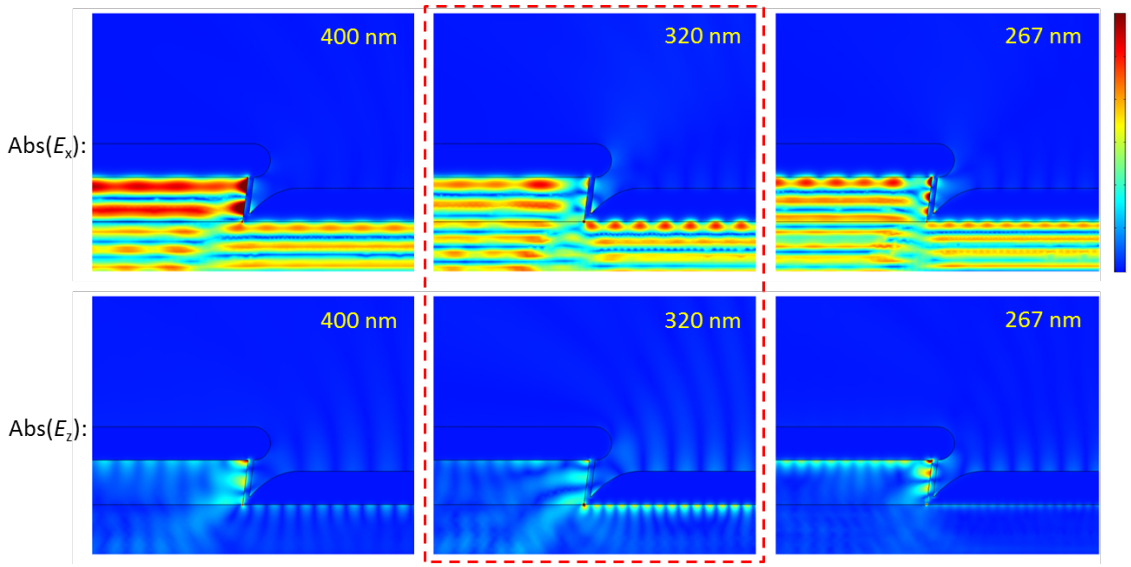

Figure S4. Simulated field profiles for absolute values of E_z and E_x at a Ag/PMMA interface for SPP wavelengths on (267 and 400 nm) and off (320 nm) resonance. On resonance, SPP standing waves form at the side wall, leading to transmission suppression. On the contrary, no standing wave forms off resonance, yielding higher transmission (brighter vertical white lines). The linear color scale ranges from 0 to 3 V/m. Trench size corresponds to circular structure with radius of 1.6 µm.

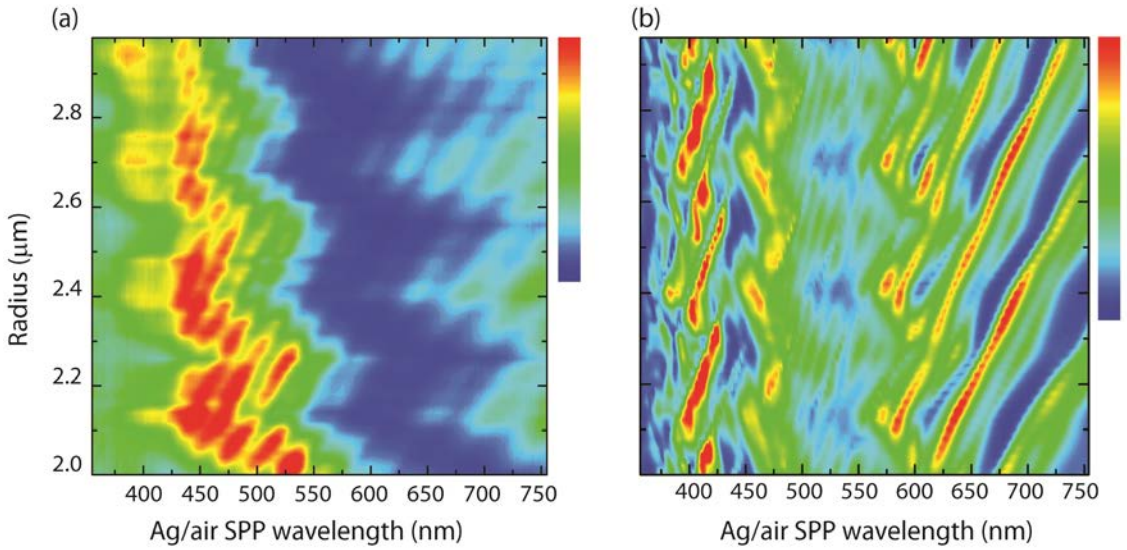

Figure S5. (a) Measured transmission spectrum contour map *vs.* SPP wavelength at the Ag/air interface for radii from 2.0 to 3.0 μm, on a PMMA layer with linearly changing height. (b) Simulated transmission spectrum contour map for the trench with width tuned from 2.0 to 3.0 μm, on a PMMA layer with linearly changing height.